RESEARCH ARTICLE

Synthesis and Characterization of Pure and Mg Doped Hydroxyapatite Nanoparticles for Orthopaedic and Dental Applications

M. Nandhini, K. Surya, V.Kalaiselvi, N. Vidhya, V.Ramya

Department of Physics, Navarasam Arts and Science Collage for Women, Erode, Tamilnadu, India

ABSTRACT: In the present study pure hydroxyapatite (HAp) and Magnesium (Mg) doped hydroxyapatite (HAp) powders were prepared by using chemical precipitation method. The samples were characterized by XRD, FT-IR, SEM, EDAX, UV and PL. The Scanning electron microscopy (SEM) and X-ray diffraction (XRD) were performed to analyze the morphology and crystal structure of Pure Mg and Mg Doped Hydroxyapatite nanoparticles, respectively.The results of Fourier Transform Infrared Spectroscopy (FT-IR) provides information on the presence of functional groups present in the synthesized sample. Morphological structure and purity of the samples were analysed by scanning Electron microscopy (SEM) and Energy Dispersion X-ray Diffraction (EDAX) techniques. The optical properties were carried out by Ultra Violet spectroscopy (UV) and Photo Luminance Spectroscopy (PL). The XRD spectra confirmed that the Mg doped Hap nanoparticles have polycrystalline hexagonal structure and crystallite size in the range.

KEYWORDS: Hydroxyapatite, Mg doped Hydroxyapatite, nanoparticles, Optical properties, Chemical precipitation

https://doi.org/10.29294/IJASE.7.2.2020.1700-1705 **© 2020 Mahendrapublications.com, All rights reserved**

1. INTRODUCTION

Synthetic hydroxyapatite being chemically similar to the inorganic constituent of bone mineral and owing to its excellent biocompatibility has been studied extensively as a bone replacement material. The use of synthetic HAp is, however, limited to low load bearing applications due to its inferior mechanical properties compared to cortical bone. Further, bone is a composite of an organic and an inorganic constituent [1].The bone-bonding ability of the material contributes to an earlier new bone apposition and clinically to higher retention of implants. HAp is extensively used in dentistry and orthopaedics applications [2]. HAp is a calcium phosphate based bio ceramic material which makes up the majority of the inorganic components of human bones and teeth [3].

Magnesium is a fundamental element and prevents possible risk factors for osteoporosis in humans [4]. Magnesium is a well-known cationic substitution in the HAP lattice 7 Magnesium ions help in bone mineralization through osteoblasts and osteoblasts activities. The amount of Mg addition has an inhibitory effect on HAP nucleation, growth, and stabilizes more acidic precursors [5].

The present work is focused on the synthesis of Mg doped HAp by cationic substitution of Mg2+ ions in the HAp lattice through chemical precipitation method. The chemical synthesized hydroxyapatite nanoparticles will be used as a best candidate as coating material for orthopaedic and dental implementations.

2. MATERIALS & METHODS

2.1 Chemical Synthesis of Mg dopped HAp

Calcium hydroxide (Ca(OH)2), Orthophosphoric acid (H3PO4), Magnesium choloride ($MgCl_2$) sodium hydroxide (NaOH) were received from Merck, Mumbai, India and used without further purifications. About 0.1 M of magnesium chloride with 50ml distilled water was taken in a beaker that was stirred for ½ hour. About 0.6 M of calcium hydroxide and 2.94ml orthophoric acid were taken in separate beakers with mixture of 50 ml distilled water and stirred for half hour. After, orthophoric acid solution was added drop wise into the calcium hydroxide solution. Then the mixture was stirred for 30 minute. Finally, the magnesium chloride was added to Hap solution with continuous stirring for 30 minutes. Then, NaOH solution was added to the solution drop by drop until the PH reaches to 12.Thus prepared solution was aged for 24 hours at room temperature. And then the precipitate was washed with deionised water to remove the impurities. The collected precipitate was dried for 45 minutes by using microwave oven at 70 watts. The dried cake was grained by using mortar in 30 minutes.

**Corresponding Authors: nandhinimahadevan0709@gmail.com & suryaaprabhu26@gmail.com*
Received: 05.09.2020 **Accepted:** 25.10.2020 **Published on**: 01.11.2020

About 1 M of Ca(OH)2 and 0.6 MH_3PO_4 were taken in separate beakers and mixed with 50 ml of extract with continuous stirring for 30 minute at room temperature. Then H_3PO_4 solution was added drop by drop into calcium hydroxide Ca(OH)2 solution and then stirred about half an hour. After that, NaOH solution was added drop by drop with continuous stirring until to reach pH reaches to 12.Thus prepared solution was aged for 24 hours at room temperature. Finally, the precipitate was washed with deionised water to remove the impurities. Then the collected precipitate was dried using microwave oven at 70 watts. The dried material was grained using mortar.

2.2 CHARACTERIZATION TECHNIQUES

2.2.1 FT-IR

Functional groups of prepared samples were identified using Fourier transform spectroscopy analysis. The spectrum was recorded in the range of 4000-400 cm-1 region [6].

2.2.2 XRD Analysis

XRD analysis is useful to determine the crystalline nature and phase identification of the nanoparticles. XRD pattern generally predicts the lattice (a & c), unit cell volume and crystalline size of the sample. The XRD pattern of prepared samples was well matched with JCPDS card no: 09-0432 (which is corresponding to hexagonal phase).

The lattice parameter of the sample was calculated using the following equation:

$$1/d2 = (4(h2+hk+K2)/3a2) + (l2/c2))$$

Where, d is the plane spacing, a and c are the lattice parameters which confirms the hexagonal structure [7].

The unit cell volume (V) of the sample was described using the given equation:

$$V= (\sqrt{3}/2) + a2+c2$$

The average crystalline size of the sample was determinedby using the Scherer's formula.

$$D = K\lambda/\beta\cos\theta$$

Where D denotes the average crystalline size of the sample, K represents the broadening constant, λ denotes the wavelength of CuKα radiation source (1.54A°), β represents the full with at half maximum, and angle of diffraction is denoted by θ[8].

2.2.3 SEM and EDAX

The surface morphologies of the synthesised HAp samples were analysed using Scanning Electron Microscopic analysis (SEM). Energy dispersive spectroscopy is used to identify the elemental composition of the sample [9].

2.2.4 Ultraviolet-Visible Spectroscopy (UV/Vis)

UV-Vis spectroscopy was used to analyze the molecular (organic) and ionic species capable of absorbing at Ultra violet wavelengths in dilute solutions [10,11].

2.2.5 Photo Luminescence Spectroscopy (PL)

Photoluminescence spectroscopy is a contactless, flexible, powerful optical method of searching the electronic structure of materials. Light is focussed on a sample, the excess energy is absorbed into the material is called photo-excitation [10].

3. RESULTS & DISCUSSION

3.1 FT-IR Spectroscopy

The FT-IR spectrum of HAp and Mg doped HAp shows the vibration modes of phosphate at 1049.32 cm^{-1} and 1041.37cm^{-1}. The peaks of Hydroxyl groups of HAp and pure HAp observed at 3747.26 cm^{-1} and 3726.20 cm^{-1}. The observed peaks of HAp and Mg doped HAp at 1498.95 cm^{-1} and 1464.47cm^{-1} represents the CH3 stretching of carboxylic acid. The results of FT-IR of HAp and Mg doped Hap are reported in Table 1 and Figure 1.

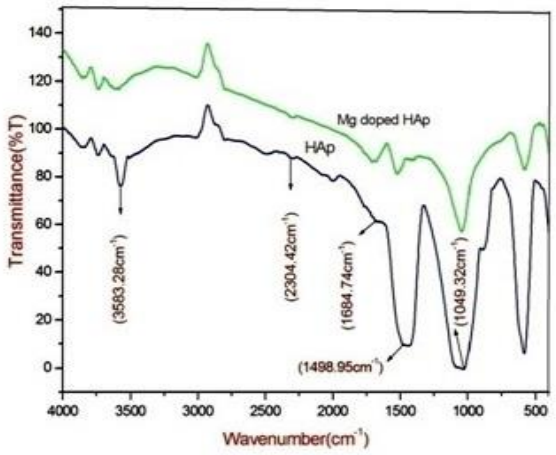

Figure 1: FT-IR spectra of pure HAp and Mg dopped Hap

3.2 XRD Analysis

The XRD pattern of pure HAp and Mg doped Hap nanoparticles were shown in Figure 2. From the XRD pattern it was clearly seen that the pure HAp and Mg

doped HAp samples are hexagonal structure and it well matched with JCPDS card number 09-0432. The average grain size of pure HAp and Mg doped HAp is 15.2 and 16.8. In the XRD analysis, four distinct peaks for pure Hap are observed at 2θ=25.84˚, 31.97˚,49.50˚, 50.72˚ and Mg doped HAp at 2θ=26.84˚, 32.97˚, 49.50˚, 50.72˚ have obtained, which is having planes of pure Hap and Mg doped HAp for 201, 112, 213 and 321 respectively.

Table 1 Functional groups of HAp and Mg doped HAp

Sample Name	Wave number (cm^{-1})				
	O-H Stretching Vibration	C-H Stretching Vibration	C=C Stretching Vibration	CH3 Bending Vibration	P-O Stretching Vibration
HAp	3747.26	2304.42	1684.74	1498.95	1049.32
Mg-doped HAp	3726.20	2310.69	1696.78	1464.47	1041.37

Table 2 The results of XRD analysis of HAp and Mg doped Hap

Sample Name	2θ (deg)	FWHM (deg)	D (Å)	Intensity (Counts)	Crystalline Size (nm)	hkl	Lattice Constant		Unit Cell Volume ($Å^3$)
							a=b	C	
HAp	25.84 31.97 49.50 50.72	0.56 0.72 0.52 0.58	3.87 2.79 1.83 1.79	68 226 56 29	14.78 11.47 16.55 15.06	201 112 213 321	9.18 9.58 9.38 9.37	6.89 6.20 6.89 6.94	516.56
Mg doped HAp	25.60 31.04 49.82 50.50	1.05 1.80 2.95 0.8	3.41 1.80 2.95 0.8	30 109 22 31	7.77 45.85 2.98 10.98	201 112 213 321	9.07 9.52 9.23 9.23	6.91 6.89 6.89 6.05	496.92

3.3 SEM and EDAX

The morphological structure of the prepared nanoparticle was studied using SEM analysis. The synthesized micrographs of pure HAp and Mg doped HAp nanoparticles were crystalline in nature. Fig 6.3 pure HAp (a) shows the needle structure and (b) shows the Mg dopedHAp reveals the small cluster like nano structure. The particle size of the pure HAp was 51.04nm to 71.72nm in diameter and Mg doped HAp was 47.27to 56.80 nm in diameter.

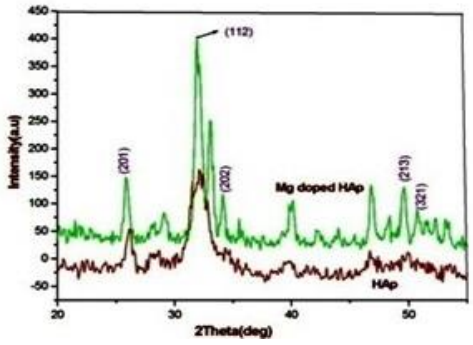

Figure 2: XRD pattern for HAp and Mg dopped Hap

The EDX analysis of pure HAp and Mg doped HAp is shown in Figure 4. The functional groups of Ca, P and o are present in the sample.EDX analysis of pure HAp and Mg doped HAp nanoparticles are shown in Table 3.

3.4 UV Analysis

UV -Vis spectroscopy investigates the optical properties and band gap energy of the sample. The absorption spectra of HAp and Mg doped HAp nanoparticles are found in the wavelength range of 302nm. The band gap energy of Hap and Mg doped HAp was 4.10eV. Table 3 shows the energy band and wavelength of the particles. Spectrum of HAp and Mg doped HAp was shown in Fig.5.

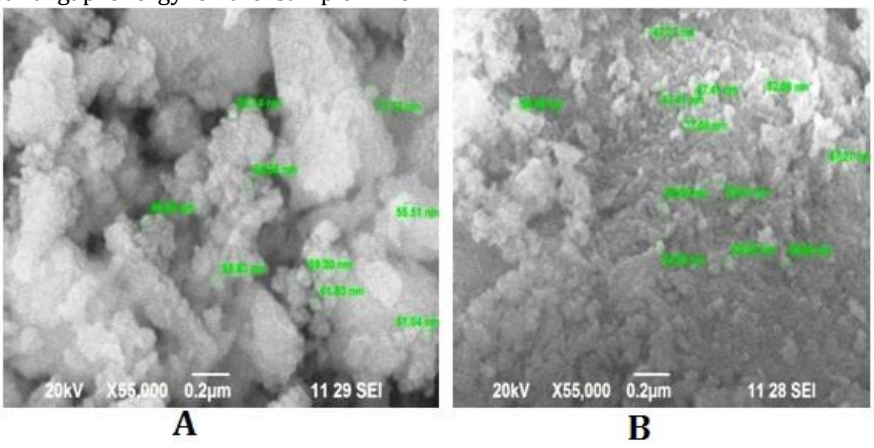

Figure 3: SEM analysis of HAp (a) and Mg dopped HAp (b)

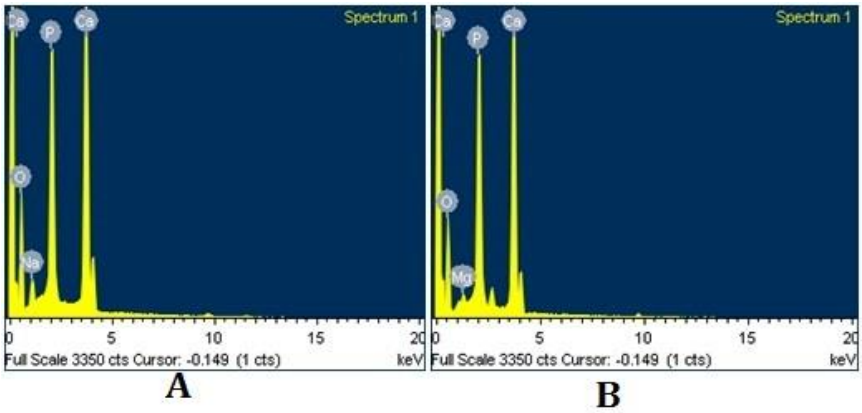

Figure 4: EDAX analysis of HAp (a) and Mg dopped HAp (b)

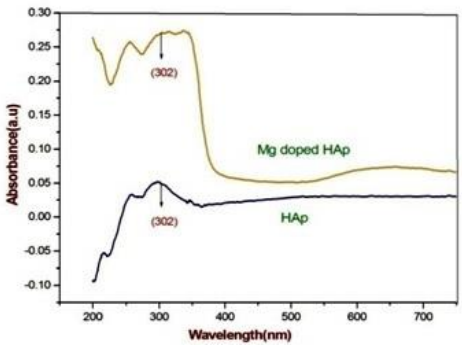

Figure 5: UV–Vis spectrum of HAp and Mg doped Hap

Table 3: Wavelength and band gap energy of HAp and Mg doped HAp

Sample name	Wavelength (nm)	Band gap energy (eV)
HAp	302	4.10
Mg doped HAp	302	4.10

3.5 Photoluminescence Spectroscopy

The intensity of emission radiations was absorbed by photoluminescence spectroscopy. The emission radiation of HAp and Mg doped HAp are shown in Figure 6. The emission band of Mg doped HAp located at 343 nm. In HAp, there was no shift present at the range. The intensity peaks increased, Due to the addition of Mg doped HAp. The standard band gap energy of HAp around the range 3.45 eV to 5.40 eV,while The calculated band gap energy of both the samples are 4.10ev.

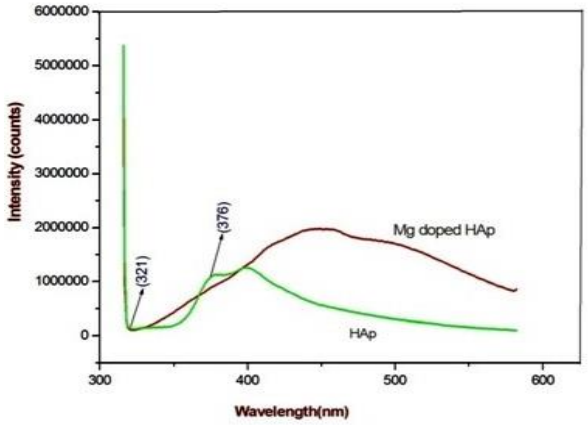

Figure 6: Photoluminescence spectra of HAp and Mg doped HAp

CONCLUSION

Hydroxyapatite nanoparticles were synthesized by chemical precipitation method and irradiated by Microwave irradiation method. The FT-IR spectrum reveals presence of functional groups. It confirms the phosphate and hydroxyl groups present in the sample. The XRD pattern confirmed the crystalline size of the sample, lattice parameter, and unit cell volume of nanoparticles. The crystalline size pure HAP in Mg doped HAp when compared with HAp. SEM analysis predicts the cluster shaped morphological structure. EDAX analysis confirms the presence of calcium and phosphate groups in the ratio of 6.84. The band gap energy and wavelength was determined from UV analysis. The band gap energy of HAp and Mg doped HAp was 4.10eV. UV and PL analysis reveals the band gap energy and optical absorption of the sample. Finally, we concluded that chemical synthesized Magnesium doped hydroxyapatite nanoparticles can be used as a best candidate for orthopaedic and dental implant.

REFERENCES

[1] Rao RR, Kannan TS. 2002. Synthesis and sintering of hydroxyapatite–zirconia composites. Materials Science and Engineering: C. May 31;20(1-2):187-93.

[2] Kalaiselvi,V, Mathamma,l R.2018. Synthesis and Characterization of Pure and Triethanolamine Capped Hydroxyapatite Nanoparticles and its Antimicrobial and Cytotoxic Activities. Asian Journal of Chemistry. 30(8):1696-700.

[3] Li J, Fartash B, Hermansson L. 1995. Hydroxyapatite-alumina composites and bone-bonding. Biomaterials. Jan 1;16(5):417-22.

[4] Kalaiselvi V, Mathammal R, Vidhya N, Surya K. 2019. Synthesis and Characterization of Pure and Capped Hydroxyapatite Nanoparticles, Int. J. Adv. Sci. Eng. 6 (1) 1213-1219

[5] Bogdanoviciene I, Beganskiene A, Tonsuaadu K, Glaser J, Meyer HJ, Kareiva A.2006. Calcium hydroxyapatite, Ca10 (PO4) 6 (OH) 2 ceramics prepared by aqueous sol–gel processing. Materials Research Bulletin. Sep 14;41(9):1754-62.

[6] Kalaiselvi V, Mathammal R, Vijayakumar S, Vaseeharan B. 2018. Microwave assisted green synthesis of Hydroxyapatite nanorods using Moringa oleifera flower extract and its antimicrobial applications. International journal of veterinary science and medicine. Dec 1;6(2):286-95.

[7] Aina V, Lusvardi G, Annaz B, Gibson IR, Imrie FE, Malavasi G, Menabue L, Cerrato G, Martra G. 2012.Magnesium-and strontium-co-substituted hydroxyapatite: the effects of doped-ions on the structure and chemico-physical properties. Journal of Materials Science: Materials in Medicine. Dec 1;23(12):2867-79.

[8] Kalaiselvi V, Mathammal R, Anitha P.2017. Sol-gel mediated synthesis of pure hydroxyapatite at different temperatures and silver substituted hydroxyapatite for biomedical applications. J Biotechnol Biomater. 7(275):2.

[9] Singh J, Singh H, Batra U. Magnesium doped hydroxyapatite: Synthesis, characterization and bioactivity evaluation. Biomaterials Science: Processing, Properties, and Applications V: Ceramic Transactions; Narayan, R., Bose, S., Bandyopadhyay, A., Eds. Sep 4:161-74.

[10] Kalaiselvi, V, Mathammal, R. 2016. Effect of Titanium Dioxide Doping on Nano Hydroxyapatite synthesised from egg shells via wet chemical Method. Int. J. Mag. Eng. Technol. Manag. Res. 3(8):133-8.

[11] Ranjitha,S, Rajarajan, G., Aroulmoji, V., Hariharan, V. , Anbarasan. P. M. 2017. Synthesis and Fabrication of Dye Sensitized Solar Cells based on ZnO and TiO_2 Nano Composites. Int. J. Adv. Sci. Eng. 4(1) 502-511

All © 2020 are reserved by International Journal of Advanced Science and Engineering. This Journal is licensed under a Creative Commons Attribution-Non Commercial-ShareAlike 3.0 Unported License.